Inorganic Chemistry

Article

pubs.acs.org/IC

A Hydrogen-Evolving $Ni(P_2N_2)_2$ Electrocatalyst Covalently Attached to a Glassy Carbon Electrode: Preparation, Characterization, and Catalysis. Comparisons with the Homogeneous Analogue

Atanu K. Das,[†] Mark H. Engelhard,[‡] R. Morris Bullock,[†] and John A. S. Roberts*[,†]

[†]Center for Molecular Electrocatalysis, Physical Sciences Division, K2-57, Pacific Northwest National Laboratory, P.O. Box 999, Richland, Washington 99352, United States

[‡]Environmental Molecular Sciences Laboratory, Pacific Northwest National Laboratory, Richland, Washington 99352, United States

Supporting Information

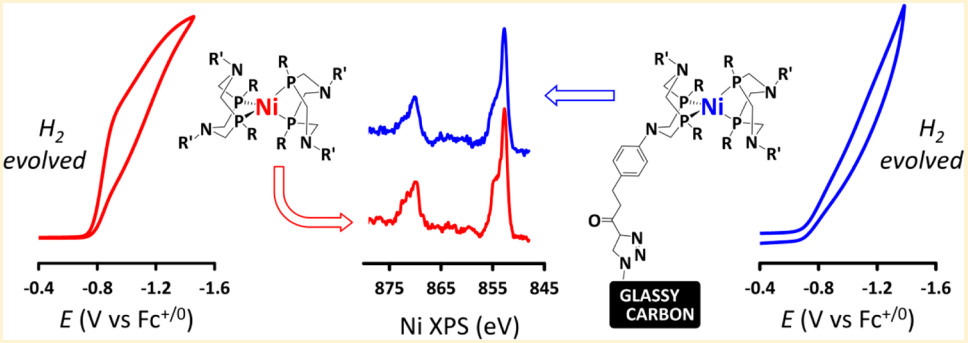

ABSTRACT: A hydrogen-evolving homogeneous $Ni(P_2N_2)_2$ electrocatalyst with peripheral ester groups has been covalently attached to a 1,2,3-triazolyllithium-terminated planar glassy carbon electrode surface. Coupling proceeds with both the Ni(0) and the Ni(II) complexes. X-ray photoemission spectra show excellent agreement between the Ni(0) coupling product and its parent complex, and voltammetry of the surface-confined system shows that a single species predominates with a surface density of 1.3×10^{-10} mol cm^{-2}, approaching the value estimated for a densely packed monolayer. With the Ni(II) system, both photoemission and voltammetric data show speciation to unidentified products on coupling, and the surface density is 6.7×10^{-11} mol cm^{-2}. The surface-confined Ni(0) complex is an electroctalyst for hydrogen evolution, showing the onset of catalytic current at the same potential as the soluble parent complex. Decomposition of the surface-confined species is observed in acidic acetonitrile. This is interpreted to reflect the lability of the Ni(II)−phosphine interaction and the basicity of the free phosphine and bears on concurrent efforts to implement surface-confined $Ni(P_2N_2)_2$ complexes in electrochemical or photoelectrochemical devices.

INTRODUCTION

Multiproton, multielectron reactions at electrode−solution interfaces are the basis for the interconversion of electrical energy with chemical fuels, transformations that figure significantly in our prospects for the development of sustainable, cost-effective energy technologies. A wide variety of homogeneous catalyst platforms have now been developed for these reactions.[1] Progress in this area has been accelerated by synthetic access to large families of catalysts with systematic structural and electronic variations that provide insights into reaction mechanisms and by a wide array of spectroscopic and computational tools. Recognition of the promise these advances hold for flow reactors such as PEM fuel cells has spurred efforts to confine homogeneous electrocatalysts based on Re,[2] Ru,[3] Rh,[2b] Co,[4] Cu,[5] and other metal systems to electrode surfaces. The $Ni(P^R_2N^{R'}_2)_2$ family of hydrogen evolution and oxidation electrocatalysts (Scheme 1; $P^R_2N^{R'}_2$ = 1,5-R′$_2$-3,7-R$_2$-1,5-diaza-3,7-diphosphacyclooctane, R, R′ = various aryl and alkyl substituents) has been targeted by several groups for both electrochemical[6] and photoelectrochemical catalysis.[7] These systems are compelling in the synthetic flexibility of the ligand platform,[8] the detail with which the catalyst structure−function relationships have been determined,[1f,9] and the fact that they are based on an earth-abundant element,[10] in this case Ni.

Some of these systems show remarkable catalytic activity, and turnover frequencies exeeding 10^4 s^{-1} for H_2 evolution have been reported.[11] Provided similar turnover frequencies can be achieved in a surface-confined catalyst on a planar electrode, achieving a benchmark current density of 20 mA cm^{-2} [12] would require a catalyst surface density of approximately 10^{-11} mol catalyst cm^{-2}, an achievable goal given that catalysts of this class are typically on the order of 10−12 Å in diameter and could pack into a monolayer having a surface density in excess of 10^{-10} mol of catalyst cm^{-2}. That catalyst performance is retained following surface attachment is by no means

Received: March 25, 2014
Published: June 7, 2014

   dx.doi.org/10.1021/ic500701a | Inorg. Chem. 2014, 53, 6875−6885

Scheme 1. Synthetic Route for Covalent Attachment of $Ni^0(P^{Ph}{}_2N^{ArNHS}{}_2)_2$ to a Glassy Carbon Surface

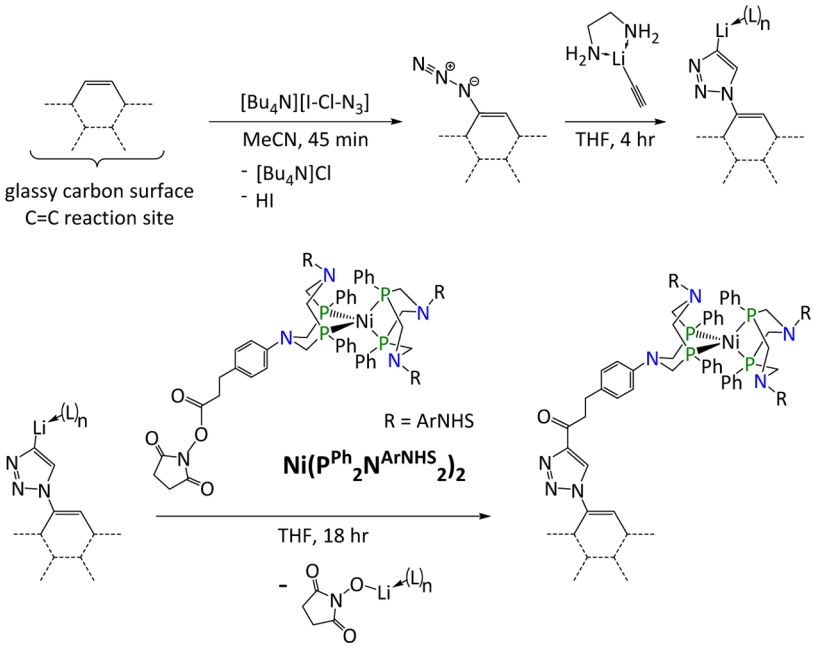

guaranteed, and characterizing surface-confined catalysts with the spatial and temporal resolution achievable with soluble species poses significant challenges.

We have approached this problem with the aim of enabling direct comparisons with homogeneous catalysts, employing the same conditions for homogeneous and surface-confined catalysts. These parameters include the electrode material (glassy carbon), its configuration (a planar surface), and the reaction medium (in the present case, acetonitrile electrolyte solution acidified with protonated dimethylformamide as the triflate salt). With these parameters fixed, the effects of surface confinement on catalyst performance and stability may be determined independently of other effects such as electrode surface morphology, reaction medium, and the use of membranes to separate the catalyst species from the acidic solution.[6]

Synthetic routes to well-defined surface linkages are a necessary prerequisite to addressing questions regarding the structure and dynamics of electrode-confined catalysts. Herein we report the covalent attachment of a $Ni(P_2N_2)_2$ complex functionalized with activated esters to a glassy carbon surface terminated by organolithium anchor points (Scheme 1). We compare the voltammetric responses and X-ray photoelectron spectroscopic data of similarly attached Ni(0) and Ni(II) species, using the authentic complexes without covalent attachment as controls. We also compare the catalytic performance of the surface-attached Ni(0) complex as a "single-site" heterogeneous electrocatalyst in acidic acetonitrile solution with that of the homogeneous parent complex. Such direct comparisons have been noted as among the primary challenges in developing and evaluating tethered single-site electrocatalysts.[13]

RESULTS

Preparation of $Ni^0(P^{Ph}{}_2N^{ArNHS}{}_2)_2$ and $[(MeCN)Ni^{II}(P^{Ph}{}_2N^{ArNHS}{}_2)_2](BF_4)_2$. The $P^{Ph}{}_2N^{ArNHS}{}_2$ ligand was prepared by esterifying the dicarboxylic acid precursor $P^{Ph}{}_2N^{ArCOOH}{}_2$ (ArCOOH = 4-$C_6H_4(CH_2)_2C(O)OH$) using *N*-hydroxysuccinimide. The Ni(0) complex $Ni^0(P^{Ph}{}_2N^{ArNHS}{}_2)_2$ was prepared by metalation of 2 equiv of the $P^{Ph}{}_2N^{ArNHS}{}_2$ ligand with Ni(1,5-cyclooctadiene)$_2$ in THF, while the Ni(II) complex $[(MeCN)Ni^{II}(P^{Ph}{}_2N^{ArNHS}{}_2)_2](BF_4)_2$ was synthesized by the reaction of $P^{Ph}{}_2N^{ArNHS}{}_2$ with $[Ni(MeCN)_6](BF_4)_2$ in MeCN. There was no sign of hydrolysis of the ester during metalation. Synthetic procedures and characterization details are presented in the Experimental Section.

Cyclic voltammetry (CV) of $[(MeCN)Ni^{II}(P^{Ph}{}_2N^{ArNHS}{}_2)_2](BF_4)_2$ in MeCN (0.1 M $[Bu_4N]PF_6$) (Figure 1A) exhibits two reversible one-electron waves corresponding to the Ni(II/I) and Ni(I/0) redox couples ($E_{1/2}$ = −0.85 and −1.04 V vs $Fc^{+/0}$, the half-wave potential of the ferrocenium/ferrocene couple and the potential of reference used throughout this paper), consistent with related Ni bis(diphosphine) complexes.[8a] $Ni^0(P^{Ph}{}_2N^{ArNHS}{}_2)_2$ shows identical Ni(II/I) and Ni(I/0) half-wave potentials (Supporting Information, Figure S1). Like related $Ni(P^R{}_2N^{R'}{}_2)_2$ complexes, these complexes are homogeneous electrocatalysts for H_2 production in MeCN (0.1 M $[Bu_4N]PF_6$) acidified with [(DMF)H]OTf (protonated dimethylformamide as the triflate salt).[14] The Ni(II) complex shows a turnover frequency (TOF) of 540 s^{-1} at 22 °C with added acid (0.35 M) and 1900 s^{-1} with 0.35 M acid +1.11 M water (Figure 1B; turnover frequencies were determined by the method reported in ref 8a). The overpotential at $E_{cat/2}$ was 0.70 V (determined as shown in ref 15). Turnover frequencies[8a] and overpotentials[15] are similar to those of related $Ni(P^R{}_2N^{R'}{}_2)_2$ complexes studied under these conditions. Acidifying a solution of the Ni(0) complex caused the color to change from pale yellow to orange, consistent with conversion to the Ni(II) salt, as expected for protonation of a hydrogen-evolving electrocatalyst in its reduced state (voltammetry of $Ni^0(P^{Ph}{}_2N^{ArNHS}{}_2)_2$ in acidic MeCN is given in Figure S2 of the Supporting Information).

Covalent Modification of Glassy Carbon with $Ni^0(P^{Ph}{}_2N^{ArNHS}{}_2)_2$ and $[(MeCN)Ni^{II}(P^{Ph}{}_2N^{ArNHS}{}_2)_2](BF_4)_2$. Glassy carbon electrodes were activated by installing 1,2,3-triazolyllithium groups as described previously;[16] minor

dx.doi.org/10.1021/ic500701a | Inorg. Chem. 2014, 53, 6875−6885

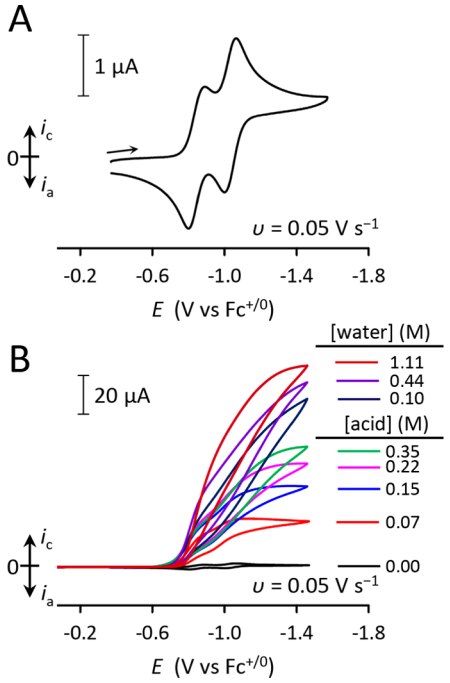

Figure 1. Cyclic voltammograms in MeCN (0.1 M $[Bu_4N]PF_6$) of $[(MeCN)Ni^{II}(P^{Ph}{}_2N^{ArNHS}{}_2)_2](BF_4)_2$ (A) with no acid added and (B) under catalytic conditions, with incremental addition of [(DMF)H]-OTf solution and subsequent incremental addition of water.

changes to the procedure are given in the Experimental Section. After activation, an electrode was held for 18 h at 22 °C in a stirred solution of $Ni^0(P^{Ph}{}_2N^{ArNHS}{}_2)_2$ (10 mM in dry THF). The electrode was then exposed to water/THF (1/10) to protonolyze the remaining organolithium anchor sites and was rinsed thoroughly with THF. Cyclic voltammograms collected in neutral MeCN (0.1 M $[Bu_4N]PF_6$) are shown in Figure 2A (scan rate υ = 0.1 V s^{-1}) and Figure 2B (υ = 0.1−3.2 V s^{-1}). Peak currents i_p (uncorrected for baseline effects such as capacitance) vary linearly with υ, as expected for discrete surface-confined species (Figure 2C).[17] Modification with $[(MeCN)Ni^{II}(P^{Ph}{}_2N^{ArNHS}{}_2)_2](BF_4)_2$ was executed in a similar fashion. Corresponding voltammograms are presented in Figure 2D,E. As with the Ni(0) system, i_p values vary linearly with υ (Figure 2F).

The cyclic voltammogram (CV) collected at υ = 0.1 V s^{-1} with the Ni(0)-modified electrode shows a single oxidation wave with E_p = −0.93 V and an accompanying reduction wave with E_p = −1.16 V (midpoint potential $E_{1/2}$ = −1.05 V, separation ΔE_p = 0.23 V). The Faradaic charge passed in the cathodic wave was 0.94 times that of the anodic wave. The cathodic wave includes a minor shoulder at more negative potential than the main peak. The CV recorded at 0.1 V s^{-1} with the Ni(II)-derived electrode shows similar primary features ($E_{1/2}$ = −1.03 V, ΔE_p = 0.15 V) but with less charge passed and a larger contribution from the minor reduction wave (E_p = −1.50 V). An accompanying oxidation wave (E_p = −1.37 V) is apparent at elevated scan rates. Changing the turnaround potential from −1.85 to −1.35 V did not affect the charge passed in the major oxidation wave (Supporting Information, Figure S3). In this case the total Faradaic charge passed in the cathodic wave was 1.34 times that of the anodic wave. The collected observations indicate that the two redox couples observed with the Ni(II)-modified electrode arise from different species. These observations were reproduced in repeated coupling trials with both the Ni(II) and Ni(0) synthons, with some variation in the relative magnitudes of the major and minor features. Responses with both synthons were stable in MeCN electrolyte both on standing and with repeated scans. The stability under catalytic conditions is examined in detail below.

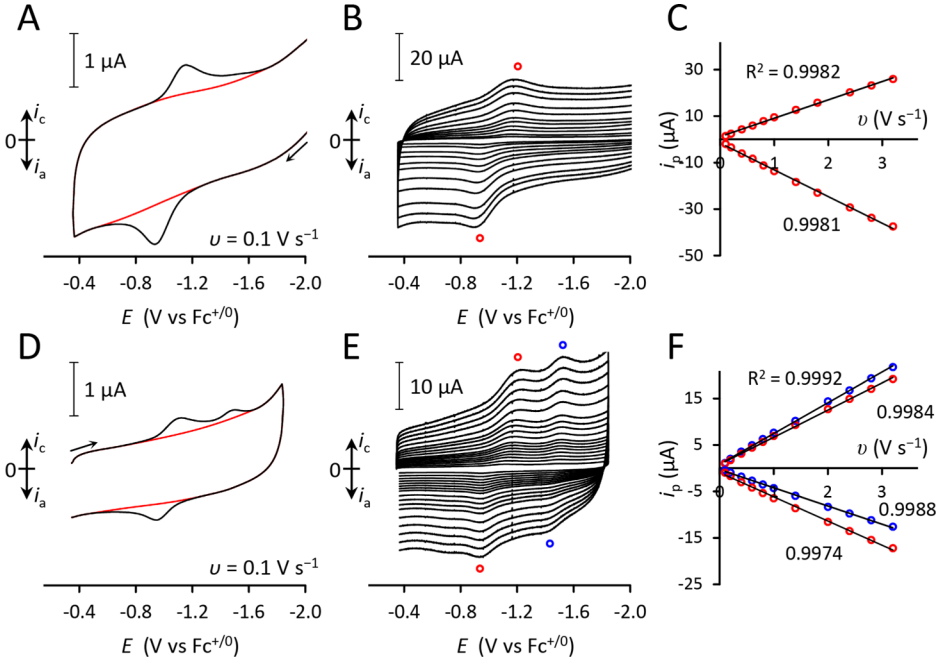

Figure 2. Voltammetric data collected in MeCN (0.1 M $[Bu_4N]PF_6$) with glassy carbon disk electrodes modified by coupling with $Ni^0(P^{Ph}{}_2N^{ArNHS}{}_2)_2$ (A−C) and $[(MeCN)Ni^{II}(P^{Ph}{}_2N^{ArNHS}{}_2)_2](BF_4)_2$ (D−F): (A, D) cyclic voltammograms with υ = 0.1 V s^{-1}, with baselines shown in red;[16] (B, E) voltammograms at different scan rates (υ = 0.1−3.2 V s^{-1});[16] (C, F) uncorrected peak currents vs scan rate.

dx.doi.org/10.1021/ic500701a | Inorg. Chem. 2014, 53, 6875−6885

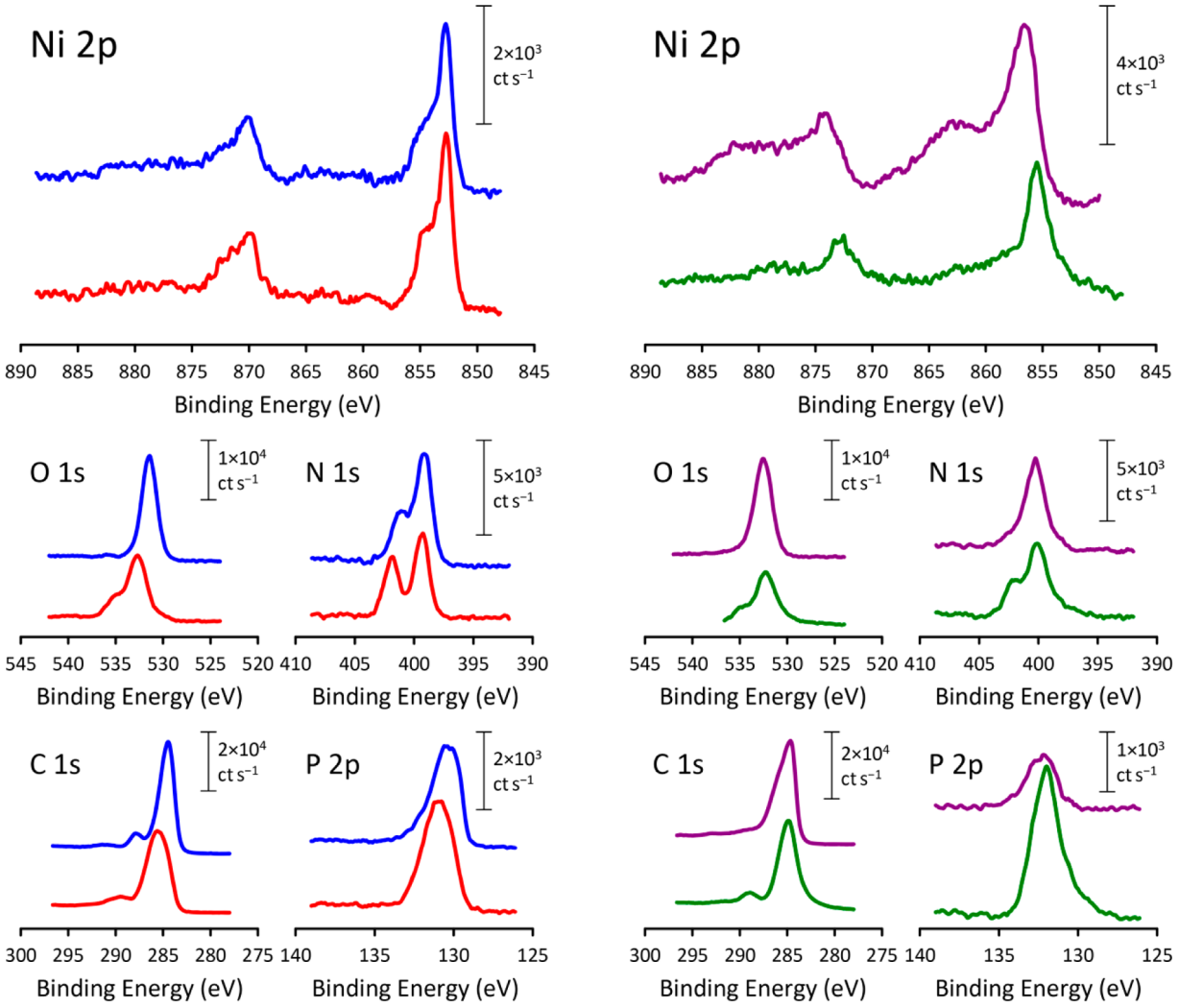

Figure 3. High-resolution photoemission spectra of glassy carbon plate samples: (left) modified with $Ni^0(P^{Ph}{}_2N^{ArNHS}{}_2)_2$ by coupling to 1,2,3-triazolyllithium surface groups (blue traces) or drop casting (red traces); (right) modified with $[(MeCN)Ni^{II}(P^{Ph}{}_2N^{ArNHS}{}_2)_2](BF_4)_2$ by coupling to 1,2,3-triazolyllithium surface groups (purple traces) or drop casting (green traces).

X-ray Photoelectron Spectroscopic (XPS) Studies. Photoemission measurements were carried out using glassy carbon plate samples modified with either the Ni(0) or Ni(II) synthon as described above. These data were compared with spectra of the authentic parent complexes, obtained by drop-casting these complexes from MeCN solution onto glassy carbon plates. Selected spectra are shown in Figure 3 (survey spectra appear in the Supporting Information, Figures S4–S7). Table 1 shows atomic abundances obtained from quantitative analyses of the XPS data. Both Ni and P are incorporated in all cases, and the measured Ni 2p binding energies are consistent with the deposition of Ni(0) and Ni(II) species, respectively, from the Ni(0) and Ni(II) coupling synthons. No samples exhibited Ni 2p photoemission lines corresponding to Ni metal (852.6 eV).[18]

XPS Results. *$Ni^0(P^{Ph}{}_2N^{ArNHS}{}_2)_2$.* As shown in Figure 3, the Ni 2p photoemission spectra of the covalently attached and drop-cast Ni(0) complexes show good agreement; the P 2p spectra are also similar. The P:Ni ratios measured with the covalently attached and drop-cast samples are 3.0:1 and 3.4:1, respectively, similar to one another and to the expected value of 4:1. The two peaks observed in the N 1s spectrum are assigned to the ligand sp^3-hybridized amine N atoms (399.1 and 399.3 eV, respectively, for the covalently attached and drop-cast samples) and the NHS imide N atoms (401.1 and 401.9 eV).[19] In the covalently attached sample, the sp^2 N atoms of the 1,2,3-triazolyl ring contribute intensity at 400.4 eV.[16,20] The residual intensity observed at 401.1 eV indicates that some NHS groups remain intact after coupling. Coupling of the ligand to the surface at more than one point is possible, however; therefore, the connectivity cannot be assigned definitively. The N:Ni ratio

Table 1. X-ray Photoelectron Spectroscopic Data[a]

preparation	atom abundance, AT%				
	C	N	O	P	Ni
1,2,3-triazolyllithium groups after protonolysis	65.5	3.7	19.7	0.1	*b*
$Ni^0(P^{Ph}{}_2N^{ArNHS}{}_2)_2$					
covalently attached	74.1	8.2	14.2	2.7	0.9
drop cast	76.5	6.6	13.0	3.1	0.9
$[(MeCN)Ni^{II}(P^{Ph}{}_2N^{ArNHS}{}_2)_2](BF_4)_2$					
covalently attached	67.6	6.3	13.3	0.9	1.3
drop-cast	70.5	8.3	8.6	2.6	0.6

[a]Average of two measurements. High-resolution photoemission spectra are presented in Figure 3. [b]None detected.

dx.doi.org/10.1021/ic500701a | *Inorg. Chem.* 2014, 53, 6875–6885

obtained with the drop-cast Ni(0) sample is 7.3:1, close to the expected value of 8:1. In the as-prepared sample, the N:Ni ratio is 9.1:1, reflecting contributions from the surface 1,2,3-triazolyl N atoms.

$[Ni^{II}(P^{Ph}{}_2N^{ArNHS}{}_2)_2](BF_4)_2$. For these samples, the primary Ni 2p photoemission lines of the covalently attached and drop-cast samples are dissimilar. The contribution to the total signal integral from the Ni 2p satellite peaks at ~863 and 880 eV is larger in the covalently attached sample than in the drop-cast sample (these overlap with the F KLL peaks from the BF_4^- counterions in both the drop-cast and covalently attached samples). The P:Ni ratio in the covalently attached sample is 0.7:1, much smaller than both the expected value of 4:1 and the value of 4.3:1 measured with the drop-cast sample. These disparities indicate substantial losses of the diphosphine ligands under coupling conditions. The new Ni(II) material may be $Ni(OH)_2$ or related species, given the similarity in energies for both the Ni $2p_{3/2}$ photoelectron (856.6 eV) and its satellite (~863 eV) to reported values[21] and given that hydroxide ions would be produced on reaction of adventitious water with unreacted 1,2,3-triazolyllithium sites. This material could also be a Ni(II) complex of the 1-oxy-2,5-pyrrolidinedione anion cleaved from the esterified ligand on coupling.

Comparison of XPS and Voltammetric Data: Coverage and Speciation. The abundances of Ni on the covalently modified surfaces were determined from XPS data[22] using the ratio of the signal integrals for the C 1s and representative Ni lines (2p for the Ni(0) synthon and 3p for the Ni(II) synthon, chosen due to overlap with the Ni 2p and F KLL lines arising from the BF_4^- counterions). Surface coverages determined by XPS were 3.5×10^{-10} mol cm^{-2} for the Ni(0) synthon and 5.5×10^{-10} mol cm^{-2} for the Ni(II) synthon. Surface coverages were also estimated using the voltammetric data. The total Faradaic charge passed was obtained by integrating the baseline-corrected responses (the baseline is shown in red in Figure 2A,D and was obtained as described previously; currents within the baseline are assigned to capacitive charging and discharging).[16] With the Ni(0)-derived system, the coverage was 1.3×10^{-10} mol cm^{-2}, determined using the data shown in Figure 2A. Repeat trials gave values ranging from 1.0 to 1.5×10^{-10} mol cm^{-2}. With the Ni(II) system, lower and upper bounds of 5.7×10^{-11} and 7.6×10^{-11} mol cm^{-2}, respectively, were calculated from the anodic and cathodic Faradaic charges passed (Figure 2D). With the Ni(II) coupling synthon, the difference in Ni coverage as determined by XPS and CV suggests that a substantial portion of the material either was rendered redox-inactive or was lost to solution prior to the CV measurement.

The coverage determined for the Ni(0) system by voltammetry is 37% of the value determined by XPS, whereas with the Ni(II) system, the coverage by voltammetry is 12% of the XPS value. Both methods carry uncertainty. The voltammetric method overestimates coverage due to the assumption that the electrode area as determined by diffusion measurements[16] is the same as the area available for binding. With the XPS method, the assumption is that the carbon signal arises exclusively from the glassy carbon support;[22] by this method the coverage is underestimated (this error decreases with decreasing actual coverage). The above comparison is valid inasmuch as these effects are the same for both the Ni(0) and Ni(II) routes.

Hydrogen Production Catalysis Results. Figure 4 compares the responses obtained using a Ni(0)-modified

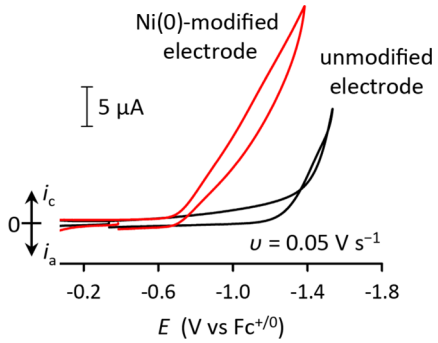

Figure 4. Cyclic voltammograms in MeCN (0.1 M $[Bu_4N]PF_6$) with acid [(DMF)H]OTf (0.66 M), recorded using a $Ni^0(P^{Ph}{}_2N^{ArNHS}{}_2)_2$-modified electrode (red trace) and using an unmodified electrode (black trace).

electrode in MeCN with added acid [(DMF)H]OTf (red trace) and an unmodified electrode under the same conditions (black trace). The increase in current with the modified electrode having an onset potential of approximately −0.71 V is assigned to the electrocatalytic production of H_2. These data demonstrate that covalent attachment of $Ni^0(P^{Ph}{}_2N^{ArNHS}{}_2)_2$ activates the electrode for catalysis at moderate potentials. Catalytic currents observed in previously reported control experiments using $[Ni(MeCN)_6]^{2+}$ in acidic MeCN showed onset potentials below −1 V vs $Fc^{+/0}$; these were assigned to H_2 evolution mediated by electrodeposited Ni metal.[23]

Figure 5 compares the response obtained with the Ni(0)-modified electrode to the response obtained with the soluble

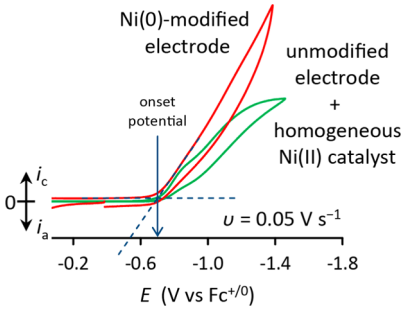

Figure 5. Cyclic voltammograms in MeCN (0.1 M $[Bu_4N]PF_6$) with acid [(DMF)H]OTf, recorded using a $Ni^0(P^{Ph}{}_2N^{ArNHS}{}_2)_2$-modified electrode (0.66 M; red trace) and using an unmodified electrode with $[(MeCN)Ni^{II}(P^{Ph}{}_2N^{ArNHS}{}_2)_2](BF_4)_2$ (0.5 mM; [acid] = 0.35 M; green trace, current axes not to scale).

Ni(II) catalyst in acid solution using an unmodified electrode (the response obtained with the soluble Ni(0) catalyst is essentially the same; see Figure S2 of the Supporting Information). The onset potentials are the same for the modified electrode and the soluble parent complex (−0.71 V).[24] This is consistent with catalysis mediated by similar species, in accord with the results obtained by XPS.

Figure 6 shows the responses obtained using the Ni(0)-modified electrode as a function of acid concentration (A) and scan rate (B). The current depends on the acid concentration up to a limiting value, as seen with homogeneous systems under similar conditions.[8a] The data shown in Figure 6B also reveal any decomposition of the catalyst. In experiments with homogeneous catalysts, the bulk solution serves as a reservoir of fresh catalyst, and so decomposition under catalytic

dx.doi.org/10.1021/ic500701a | Inorg. Chem. 2014, 53, 6875−6885

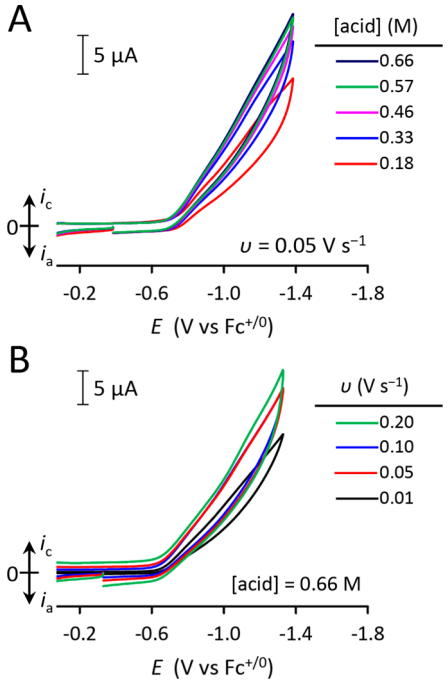

Figure 6. Cyclic voltammograms using a $Ni^0(P^{Ph}_2N^{ArNHS}_2)_2$-modified electrode in MeCN (0.1 M $[Bu_4N]PF_6$) with the acid [(DMF)H]OTf at the listed concentrations and at the scan rate υ = 0.05 V s^{-1} (A) and with 0.66 M [(DMF)H]OTf at the listed scan rates (B).

conditions cannot be quantified by CV. The current observed with 0.66 M [(DMF)H]OTf is independent of the scan rate over the range 0.05−0.2 V s^{-1}, indicating that the rate of catalysis is not limited by transport of the acid substrate to the electrode. A first-order dependence on catalyst surface coverage, Γ, was assumed by analogy with homogeneous systems,[8a,25] allowing the turnover frequency (TOF) to be calculated using the steady-state approximation represented in eq 1,[26] where n is the number of redox equivalents passed per

$$\mathrm{TOF} = \frac{i_{cat}}{nFA\Gamma} \quad (1)$$

turnover (2), F is the Faraday constant, and A is the area of the electrode (0.071 cm^2). The catalytic current i_{cat} was measured at −1.25 V, and the surface coverage, Γ, was determined by prior voltammetry with the same electrode in neutral MeCN, giving a TOF value of 28 s^{-1}. This equation assumes that catalysis is mediated by surface-confined species and that all of the species giving rise to Faradaic current in contact with neutral solution are catalytically active when in contact with acidic solution. Direct comparison of the raw CV traces collected with the homogeneous and surface-confined catalysts (Figure 5) does not accurately represent differences in turnover frequency, since this quantity depends on i_{cat}^2 for homogeneous catalysts and on i_{cat} for surface-confined catalysts.[26] While electrodes prepared using the Ni(II) complex showed some catalytic current (see Figure S8 of the Supporting Information), catalysis studies focused on electrodes prepared using the Ni(0) synthon. Adding water (0.1 M) does not change the catalytic current.

Stability of Surface-Confined Ni Species under Catalytic Conditions. As mentioned above, the surface-confined species appear stable on exposure to neutral MeCN (0.1 M $[Bu_4N]PF_6$). The voltammetric response under noncatalytic conditions is invariant with repeated scanning and does not diminish appreciably on standing for 15 min in stirred MeCN with electrolyte. Decomposition does occur in acidic solution in the absence of an applied potential: measurements in neutral MeCN (0.1 M $[Bu_4N]PF_6$) recorded before and after holding the modified electrode 15 min in stirred MeCN electrolyte acidified with [(DMF)H]OTf (0.18 M) showed a 20% decrease in peak currents for the main feature at $E_{1/2}$ = −1.05 V, although the voltammograms were otherwise similar. The scan rate independence shown in Figure 6B tentatively indicates that decay is not appreciably faster under applied potentials in comparison to that when the electrode is simply held in a stirred acidic solution. Catalyst instability in acid solution appears to be related to acid strength: $[(Et_2O)_2H]B(C_6F_5)_4$, likely a much stronger acid in MeCN than [(DMF)H]OTf (pK_a^{MeCN} = 6.1),[27] does not afford a catalytic response with the modified electrode but does lead to rapid decomposition. Decomposition also occurs with the weak acid anisidinium tetrafluoroborate (pK_a^{MeCN} = 11.86)[28] but is slower than with [(DMF)H]OTf. The catalytic response is marginal with anisidinium tetrafluoroborate, as observed with anilinium acids in MeCN in catalysis with related soluble $Ni(P_2N_2)_2$ catalysts.[8a] These data are presented in Figures S9 and S10 of the Supporting Information.

DISCUSSION

Substantial progress has been made in the surface confinement of $Ni(P_2N_2)_2$ electrocatalyst systems, for both electrocatalytic[6] and photocatalytic[7] applications; however, questions regarding the structure, function, and stability of surface species remain unanswered.[29] The intent of the present approach is to facilitate the study of surface-confined analogues of $Ni(P_2N_2)_2$ and related systems by retaining, to the greatest extent possible, both uniformity in local catalyst environments and comparability with soluble analogues. This approach should allow molecular-level aspects of electrocatalysis with surface-confined molecular systems to be considered independently of electrode configuration. For example, porous electrode materials are well-suited to flow electrocatalysis cells; however, mass or charge transport depends on electrode architecture, and may influence turnover as much as catalyst performance does. Understanding catalysis at planar electrodes can aid in the development of systems based on more complex electrode structures.

Our synthetic route (Scheme 1) begins with the production of lithiated 1,2,3-trizolyl groups at a macroscopically planar glassy carbon surface.[16] In the first step, an iodine azide equivalent adds across a surface C═C unsaturation and HI is eliminated;[20] in a second step, the surface azides are reacted with lithium acetylide−ethylenediamine.[30] Subsequent coupling of redox-active eletrophilic synthons should then generate a monolayer or submonolayer with each redox center at approximately the same distance from the glassy carbon. To our knowledge, none of these reactions proceed by a radical pathway, and given that the process involves two distinct steps, it seems unlikely that deposition of 1,2,3-triazolyllithium groups would proceed beyond a single layer. Avoiding radical intermediates should preclude nonrandom distributions of surface sites, such as for example branched structures or multilayers that can be produced with aryldiazonium coupling[31] wherein electroreduction of $[ArN_2]^+$ generates an aryl radical that couples to the electrode surface.[32] The 1,2,3-triazolyl-lithium groups couple with a variety of electrophiles,[30]

dx.doi.org/10.1021/ic500701a | Inorg. Chem. 2014, 53, 6875−6885

Table 2. Comparison of Voltammetry in Neutral Solution and Catalytic Results in Acid Solution with Surface-Confined $Ni(P_2N_2)_2$ Complexes

mode of attachment	support	$E_{1/2}$ (V vs $Fc^{+/0}$)	ΔE_p (V)[a]	Ni coverage (mol cm^{-2})	j_{cat}[b] (A cm^{-2})	TOF[c] (s^{-1})	ref
covalent, Ni(II)	planar glassy carbon	−1.03	0.15	6.7×10^{-11}	n.d.	n.d.	this work
covalent, Ni(0)	planar glassy carbon	−1.05	0.20	1.3×10^{-10}	0.71	28	this work
covalent	planar ITO[d]	−0.90	0.29	4.5×10^{-11}	n.d.	n.d.	6a
covalent	carbon nanotubes	−0.98	0.12	1.5×10^{-9}	2	7	6a
$\pi-\pi$ stacking	carbon nanotubes	−0.98	0.06	2×10^{-9}	4.2	11	6b

[a]Peak-to-peak separation; for Nernstian electron transfer with surface confined species this value approaches 0. [b]Catalytic current density. [c]Turnover frequency. [d]Indium tin oxide.

including activated esters,[33] which are easily accessed from carboxylic acids as we have done in the present case using *N*-hydroxysuccinimide (NHS). Other electrophilic coupling synthons may be used: we have reported coupling of ferrocenyl groups with terminal iodo- and bromoalkanes and aldehydes.[16]

While surface confinement proceeds with esterified complexes of both Ni(II) and Ni(0), we have found that coupling is much cleaner with the Ni(0) synthon. The voltammetry obtained with the Ni(II) congener in neutral electrolyte solution shows a second quasi-reversible redox system at a more negative potential (Figure 2D). Its origin is unknown, though XPS measurements indicate that much of the Ni deposited on the surface is not in a bis(diphosphine) bonding environment. This unwanted reactivity with Ni(II) may be related to the generation of hydroxide from adventitious water under the coupling conditions. Our pursuit of the Ni(0) coupling strategy was motivated by the hypothesis that the comparatively Lewis acidic Ni(II) complex was itself susceptible to nucleophilic attack. This may may be relevant to other coupling strategies involving strong bases.

The voltammetry obtained with the Ni(0)-modified electrode in neutral MeCN shows a single feature with $E_{1/2}$ = −1.05 V vs $Fc^{+/0}$, close to the potential of the parent Ni(I/0) couple (−1.04 V). The response is substantially similar in this regard to results reported by Artero and co-workers in their work with $[Ni^{II}(P_2N_2)_2]^{2+}$ systems attached either by covalent bonds[6a] or by $\pi-\pi$ stacking.[6b] These results are compared with our own in Table 2. For all of the surface-confined species given, the homogeneous analogues show two well-separated one-electron waves typical of Ni bis(diphosphine) complexes, with Ni(II/I) couples ranging from $E_{1/2}$ = −0.74 to −0.85 V vs $Fc^{+/0}$ and Ni(I/0) couples ranging from −0.93 to −1.04 V.[6] In each case, the surface-confined system affords a single redox feature near the Ni(I/0) couple of the parent species.

Artero and co-workers assigned this single feature to an overall two-electron redox process,[6,34] and we concur with their assignment. The effect of surface confinement on the stoichiometric voltammetry may originate in changes in preferred coordination geometry with oxidation state. All of the structurally characterized $[Ni^{II}(P_2N_2)_2]^{2+}$ complexes are either distorted square planar[8a,25,35] or trigonal bipyramidal with a dative ligand (MeCN,[8b,25,36] CO or cyclohexyl isocyanide,[37] or acetate[36b]) in the equatorial plane,[8b,25,36,37] with instances of both four- and five-coordinate Ni(II) species measured in two cases (R = Ph, R′ = 4-$MeOC_6H_4$[8a,36b] with MeCN and R = Cy, R′ = Bn with CO or cyclohexyl isocyanide[25,37]). Pentacoordinate $[(MeCN)Ni^{II}(P_2N_2)_2]^{2+}$ species have been characterized by NMR spectroscopy,[38] and comparison of computed Ni(II/I) redox potentials for four- and five-coordinate variants with measured values indicates that the MeCN-coordinated species predominate in solution.[39] In contrast, all of the structurally characterized Ni(I) and Ni(0) species are pseudotetrahedral.[40] The change in geometry on traversing the Ni(II/I) couple is illustrated in Scheme 2. As has been noted,[6a] coupling of more than one ester group per molecule could certainly influence this rearrangement. In the present system, varying the scan rate from 10 mV s^{-1} to 3.6 V s^{-1} did not appreciably affect the peak-to-peak separation (ΔE_p), indicating that the influence of surface confinement on the reduction of Ni(II) to Ni(I) is thermodynamic rather than kinetic in origin.

Scheme 2. Expected Changes in Coordination Geometry with Redox State for an Archetypal $Ni(P_2N_2)_2$ Complex in MeCN Solution

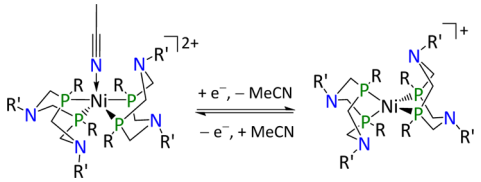

Catalysis ensues near the Ni(II/I) redox potential in the homogeneous system (Figure 1), as has been observed with related systems in acidic MeCN solution.[8] The change in relative free energies of the Ni(II) and Ni(I) states observed on surface confinement might therefore be expected to influence the catalytic response as well. However, the onset potentials for the surface-confined system and the homogeneous parent complex are the same (Figure 5). One possibility is that the Ni complex is cleaved from the electrode prior to catalysis and that the active catalyst is in fact homogeneous. We observed that the surface-confined complex is stable in acidic MeCN in the absence of an applied potential (on the time scale of a CV experiment, less than 1 min in the present studies) but somewhat less stable in acid solution. If the complex must dissociate from the electrode to become active, then the gradient in catalyst concentration extending from the electrode surface, and thus the catalytic current, should evolve with time.[41] However, the response is invariant with scan rate over a potential range of 0.6 V for scan rates ranging from 0.05 to 0.2 V s^{-1} (Figure 6B), indicating catalysis at steady state. This means that the transport of protons does not limit the rate of catalysis[42] and, more importantly in this context, that the population of active catalyst does not change on the CV time scale. While not definitive proof that catalysis is mediated solely by surface-confined species, this observation is inconsistent with a catalytic response dominated by a soluble species generated during the potential sweep.

The difference in stoichiometric and catalytic responses seen with the surface-confined system may indicate that the redox-

dx.doi.org/10.1021/ic500701a | Inorg. Chem. 2014, 53, 6875−6885

induced changes in coordination geometry for the Ni(II/I) couple under stoichiometric conditions (illustrated in Scheme 2 above) are not required for turnover. Scheme 3 presents a

Scheme 3. Intermediates in the Evolution of Hydrogen with an Archetypal $Ni(P_2N_2)_2$ Complex

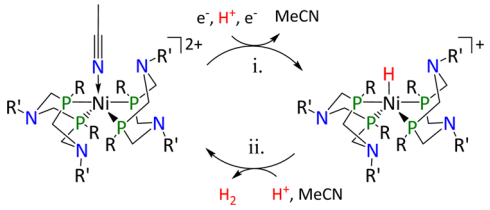

simplified mechanism for catalysis at moderate potentials: reduction to Ni(I) triggers the transfer of a proton to Ni by way of a ligand pendant amine, which occurs in conjunction with a second reduction step to produce a Ni(II) hydride[39,43] (step i). Reaction of the hydride complex with a second equivalent of acid produces the H−H bond and regenerates the Ni(II) complex (step ii; detailed mechanistic studies examining both steps i and ii along with alternative productive and nonproductive pathways have been presented[43,44]). The reduction of the tethered five-coordinate $[(MeCN)Ni^{II}(P^{Ph}_2N^{ArNHS}_2)_2]^{2+}$ in acidic solution then generates the tethered five-coordinate $[HNi^{II}(P^{Ph}_2N^{ArNHS}_2)_2]^{+}$. Analogous soluble Ni(II) hydrides are fluxional at ambient temperatures in MeCN-d_3 solution, showing a pentad ^{1}H NMR signal for the hydride and a single ^{31}P resonance[36b] that resolves to two inequivalent P resonances at low temperatures.[38] These data, along with parallel computational studies,[39] suggest that a trigonal-bipyramidal conformer with an equatorial hydride ligand as shown in Scheme 3 is thermally accessible in the homogeneous complexes at ambient temperatures. If the reactions forming this species occur in a concerted fashion, the unprotonated Ni(I) state may be short-lived or even nonexistent. In this case, the rearrangement required on reduction of Ni(II) would be less sensitive to surface confinement effects.

The observed turnover frequency is much lower with the surface-confined species than with the homogeneous analogue. This may be related to the mutual proximity of the Ni species: the measured surface coverage of Ni is 1.3×10^{-10} mol cm^{-2}, as determined by CV analysis. A molecular "footprint" approximating the minimum area A_m occupied by the molecule on the surface may be calculated from crystallographic data according to eq 2, where V_{cell} is the unit cell volume and Z is the number

$$A_m = \left(\frac{V_{cell}}{Z}\right)^{2/3} \quad (2)$$

of formula units per unit cell. Data from published structures[8,25,35−37,40] affords values of $A_{molecule}$ ranging from 94 to 152 Å^2 and averaging 132 Å^2. A packed monolayer would thus have a coverage $\Gamma = 1 \times 10^{16}/(N_A \times A_m) \approx 1.3 \times 10^{-10}$ mol cm^{-2}, suggesting that this condition is approached in the present case. Steric crowding could interfere with conformational motion in thermal steps[38] including important isomerization reactions, or with redox steps. Hamers and co-workers have reported slow electron transfer at high coverage in surface-confined ferrocenyl groups,[22a] arguing that excessively close packing limited the proximity of the redox centers to the electrode. Meyer and co-workers have noted inhibited electron transfer in surface-confined Ru(polypyridyl) complexes.[3a] Control over surface coverage may be important in the optimization of tethered molecular electrocatalysts of this class.

The primary challenge to be addressed, however, is stability under catalytic conditions. With discrete adsorbed species, the driving force for dissociation from the surface is proportional to the gradient in chemical potential of the adsorbate at the solid−solution interface[45] and is therefore substantial, at least initially, when a populated surface is placed in contact with a good solvent for the adsorbate. This is one of the fundamental differences between homogeneous and heterogeneous catalysis. Another difference pertaining to electrocatalysis in particular is that with homogeneous catalysts the bulk solution serves as a reservoir of fresh catalyst, meaning that the decomposition of species generated under catalytic conditions may not be readily detected.

Given the importance of decomposition, it is worth considering its origins in light of what is known about the homogeneous analogues. In the heteroleptic complex $[Ni(dppp)(P^{Ph}_2N^{Bz}_2)]^{2+}$ (dppp = 1,3-bis(diphenylphosphino)propane) in benzonitrile, ligand exchange producing the corresponding homoleptic complexes has been observed, indicating that the Ni(II)−phosphine dative interactions in a complex with a similar P_2N_2 ligand are labile; that work points out a paucity of isolable heteroleptics.[46] The tethered Ni(II) species is stable on standing 15 min in neutral electrolyte and also during voltammetry but decomposes on standing in acid solution. Dissociated phosphine groups may be trapped by protonation: $[(DMF)H]^+$ has a pK_a of 6.1 in MeCN,[27a] and the pK_a values of protonated triphenylphosphine and diphenylmethylphosphine are 7.61 and 9.96, respectively.[28] Protonation of the first of the two P_2N_2 phosphines on dissociation would increase the likelihood of dissociation of the other phosphine.

Decomposition of reduced catalytic intermediates is also possible. Several NMR studies have been conducted with soluble doubly protonated Ni(0) species,[9b,38,44b] and these complexes appear to be stable with respect to ligand dissociation; however, whether this is also the case for surface-confined species is an open question. The known $[HNi(P_2N_2)_2]^{2+}$ complexes are unstable in MeCN—although several have been generated in situ for electrochemical and spectroscopic measurements,[36b,46,47] they generally decompose at ambient temperatures in MeCN and only two have been isolated thus far.[40b,44b] Henderson and co-workers observed that $[HNi^{II}(dppe)_2]^+$ (dppe = $Ph_2PCH_2CH_2PPh_2$) reacts with HCl in THF to produce $[Ni^{II}(dppe)Cl_2]$, H_2, and 1 equiv of free dppe.[48] They proposed that the coordination vacancy required for binding of the Cl$^-$ ligand is created by dissociation of a Ni−P dative interaction in the hydride. Careful consideration of the kinetics of decomposition of specific intermediates may prove essential in the development of robust surface-confined $Ni(P_2N_2)_2$ electrocatalysts.

CONCLUSIONS

The esterified $Ni(P_2N_2)_2$ complex $Ni^0(P^{Ph}_2N^{ArNHS}_2)_2$ couples cleanly to a 1,2,3-triazolyllithium-terminated glassy carbon surface and produces a densely packed layer. Coupling is not as clean with the Ni(II) congener. Surface attachment changes the potential of the Ni(II/I) redox couple but not that of the Ni(I/0) couple, as measured under noncatalytic conditions; however, this does not influence the potential where catalysis is observed. The onset of catalysis at similar potentials with both the

dx.doi.org/10.1021/ic500701a | Inorg. Chem. 2014, 53, 6875−6885

surface-confined system and its homogeneous parent complex may be due to the decomposition of surface species to generate an active homogeneous catalyst. However, catalysis appears to proceed at a steady state, suggesting that the measured response arises largely from surface-confined species.

The surface-confined Ni(II) complex decomposes more rapidly in acidic solution than in neutral solution. The pathway for this decomposition may involve protonation of free phosphine groups. Another susceptible intermediate may be the surface-confined Ni(II) hydride. This intermediate is necessary for turnover in the homogeneous analogues, and soluble $[HNi^{II}(P_2N_2)_2]^+$ complexes are unstable in general. Developing durable surface-confined $Ni(P_2N_2)_2$ electrocatalysts may require a specific focus on stabilizing these Ni species.

While synthetically accessible, coupling synthons such as $Ni^0(P^{Ph}{}_2N^{ArNHS}{}_2)_2$ that attach through the pendant amine substituents may not be optimal for catalyst performance or stability. Further refinements to the coupling methodology may allow control over the surface density, distance from the electrode, and the number and disposition of anchor points, all of which may be relevant to raising the performance of tethered $Ni(P_2N_2)_2$ complexes to the level of their homogeneous counterparts. The present work demonstrates that the detailed understanding required for these advances is achievable, and that the logical abstraction furnished by studies using planar electrodes facilitates the development of this understanding.

EXPERIMENTAL SECTION

Materials and Methods. All manipulations were carried out in a N_2 glovebox unless otherwise noted. Acetonitrile (MeCN; Burdick & Jackson BioSyn), dimethylformamide (DMF; Burdick & Jackson, anhydrous), and ethylene glycol (Aldrich, anhydrous) were purified by sparging with nitrogen. Diethyl ether (Et_2O, Fisher, anhydrous, not stabilized) was purified by sparging with nitrogen and passage through neutral alumina. Tetrahydrofuran (THF; VWR, anhydrous, not stabilized) was purified by sparging with nitrogen and passage through neutral alumina and then vacuum-distilled from liquid NaK alloy. Water was dispensed from a Millipore Milli-Q purifier (18.2 MΩ cm) and sparged with nitrogen. MeCN-d_3 (Cambridge Isotope Laboratories, 99.5% D) was vacuum-distilled from P_2O_5. THF-d_8 (Cambridge Isotope Laboratories, 99.5% D) was vacuum-distilled from liquid NaK alloy. Acetone (Fisher ReagentPlus) was used as received. Ferrocene (Fc; Aldrich) was purified by sublimation. $[Bu_4N]PF_6$,[49] [(DMF)H]OTf,[14] $[Ni(MeCN)_6](BF_4)_2$,[50] and $P^{Ph}{}_2N^{ArCOOH}{}_2$ (ArCOOH = 4-$C_6H_4(CH_2)_2C(O)OH$)[51] were prepared by reported methods. $[Bu_4N][Cl{-}I{-}N_3]$ was prepared immediately prior to use as previously described[16] from as-received $[Bu_4N]N_3$ and ICl (Aldrich). Lithium acetylide−ethylenediamine complex ((en)-LiC≡CH), aqueous HCl (37%), *N*-(3-(dimethylamino)propyl)-*N*′-ethylcarbodiimide hydrochloride (EDC·HCl), *N*-hydroxysuccinamide (NHS), and Ni(1,5-cyclooctadiene)$_2$ were used as received (Aldrich).

Preparation of Glassy Carbon Substrates for Surface Modification. Glassy carbon disks (3 mm diameter) encased in poly(chlorotrifluoroethylene) (for voltammetry, BAS Instruments) and 4 × 10 × 10 mm glassy carbon plates (for XPS analysis, SPI-Glas 22 grade, SPI supplies) were lapped and polished on a mechanical wheel (Electron Microscopy Sciences Model 900) and then cleaned, as previously described.[16]

Instrumentation and Analytical Methods. XPS measurements were performed as previously described[16] using a Physical Electronics Quantera Scanning X-ray Microprobe. Glassy carbon plate samples were mounted for analysis inside a N_2 glovebox interfaced with the vacuum chamber. Spectra were referenced using the C 1s photoemission line, by fitting the raw signal using two components separated by 0.3 eV (the difference in binding energies for the sp^2 C atoms in benzene[52] and highly oriented pyrolytic graphite[53]) and setting the higher energy line at 284.8 eV and the lower energy line at 284.5 eV.

Surface densities were calculated from XPS data using the method outlined in ref 22b. The density of glassy carbon was taken as reported by the supplier (1.42 g cm^{-3}). The inelastic mean free path for the C 1s photoelectron (33.85 Å) was obtained from the Quases-IMFPTPP2M (Tanuma, Powell, Penn) material properties database, corrected for the difference in density of the glassy carbon used vs that listed in the database (1.80 g cm^{-3}).

Electrochemical measurements were conducted using a CH Instruments 620D potentiostat and a standard three-electrode cell (4 or 10 mL shell vial). The counterelectrode was a glassy carbon rod (3 mm diameter; Alfa Aesar). The reference electrode was a silver wire (1 mm diameter; 99.9%, Alfa Aesar) anodized for 5 min in aqueous HCl, washed with water and acetone, dried, and suspended in a glass tube containing neutral MeCN (0.1 M $[Bu_4N]PF_6$) and fitted with a porous Vycor disk. Fc was added as an internal potential standard for all measurements. Unmodified working electrodes (1 mm diameter; ALS) used for voltammetry of solutions of the Ni complexes and for select controls (3 mm diameter; BAS Instruments) in the study of the modified electrodes were polished with diamond paste (0.25 μm, Buehler) on a pad (Buehler MicroCloth) lubricated with ethylene glycol.

Syntheses. *$P^{Ph}{}_2N^{ArNHS}{}_2$.* In a 25 mL Schlenk flask, $P^{Ph}{}_2N^{ArCOOH}{}_2$ (213.8 mg, 0.36 mmol) and NHS (94.5 mg, 0.82 mmol) were dissolved in 10 mL of DMF. Solid EDC·HCl (157.4 mg, 0.82 mmol) was added, and the mixture was stirred for 24 h at 22 °C to afford a clear pale yellowish solution. Water (50 mL) was added, yielding a white precipitate that was filtered and washed thoroughly with cold water and dried under vacuum to give a white powder (239 mg, yield 85%). $^{31}P\{^1H\}$ NMR (THF-d_8): δ −50.79 (s). ^1H NMR (THF-d_8): δ 7.69 (br, 4H), 7.50 (m, 6H), 7.09 (d, 4H, J = 8.1 Hz), 6.73 (d, 4H, 8.2 Hz), 4.41 (m, 4H), 4.27 (m, 4H), 2.91 (m, 4H), 2.83 (m, 4H), 2.77 (s, 8H). Anal. Calcd for $C_{44}H_{44}N_4O_8P_2$: C, 63.63; H, 5.34; N, 7.07. Found: C, 63.59; H, 5.58; N, 7.20.

$[(MeCN)Ni^{II}(P^{Ph}{}_2N^{ArNHS}{}_2)_2](BF_4)_2$. A solution of $[Ni(MeCN)_6](BF_4)_2$ (34.0 mg, 0.071 mmol) in MeCN (5 mL) was added to a stirred slurry of $P^{Ph}{}_2N^{ArNHS}{}_2$ (108.6 mg, 0.137 mmol) in MeCN (5 mL), the solution changing rapidly from blue to clear orange-red. The solution was stirred overnight and then filtered through a plug of Celite. The solvent was removed under vacuum, and the residue was washed with Et_2O and dried under vacuum to give a red powder (113 mg, 90%). $^{31}P\{^1H\}$ NMR (MeCN-d_3): δ 5.28 (s). ^1H NMR (MeCN-d_3): δ 7.40 (t, J = 7.5 Hz, 7.4 Hz, 5H), 7.31 (m, 15H), 7.17 (m, 16H), 7.25−7.18 (m, 16H), 4.21 (d, J = 13.7 Hz, 8H), 3.90 (d, J = 12.3 Hz, 8H), 3.01 (d, J = 6.2 Hz, 8H), 2.98 (d, J = 6.2 Hz, 8H), 2.71 (s, 16H), 2.00 (s, 3H). Anal. Calcd for $C_{84}H_{84}B_2F_8N_8NiO_{16}P_4$: C, 55.56; H, 4.72; N, 6.78. Found: C, 54.43; H, 4.87; N, 7.25.

$Ni^0(P^{Ph}{}_2N^{ArNHS}{}_2)_2$. A yellow solution of Ni(1,5-cyclooctadiene)$_2$ (50.6 mg, 0.181 mmol) in THF (2 mL) was added to a stirred slurry of $P^{Ph}{}_2N^{ArNHS}{}_2$ (249.2 mg, 0.314 mmol) in THF (5 mL). The solution was stirred overnight and then filtered through a plug of Celite. The solvent was removed under vacuum, and the residue was purified by crystallization from MeCN/Et_2O at −35 °C. The precipitate was collected and dried under reduced pressure to give a yellow powder (223 mg, 86%). $^{31}P\{^1H\}$ NMR (THF-d_8): δ 6.31 (s). ^1H NMR (THF-d_8): δ 7.84 (br, 8H), 7.16 (t, J = 7.7 Hz, 5H), 7.17 (m, 16H), 7.10 (d, J = 8.7, 8H), 7.06 (t, J = 7.5 Hz, 7H), 6.95 (d, J = 7.3 Hz, 8H), 3.95 (d, J = 12.2 Hz, 8H), 3.60 (m, 8H), 2.92 (m, 8H), 2.84 (m, 2H), 2.73 (s, 16H). Anal. Calcd for $C_{84}H_{84}N_8NiO_{16}P_4$: C, 61.36; H, 5.15; N, 6.82. Found: C, 60.93; H, 5.29; N, 7.70.

Electrocatalysis with the Soluble Complexes $Ni^0(P^{Ph}{}_2N^{ArNHS}{}_2)_2$ and $[(MeCN)Ni^{II}(P^{Ph}{}_2N^{ArNHS}{}_2)_2](BF_4)_2$. In a representative experiment, $Ni^0(P^{Ph}{}_2N^{ArNHS}{}_2)_2$ (1.9 mg, 1.2 μmol) was weighed into the cell and dissolved in 2 mL of MeCN (0.1 M $[Bu_4N]PF_6$). Fc was added, and a CV spanning the $Fc^{+/0}$ reference couple and both the Ni(II/I) and Ni(I/0) couples was recorded. In a separate vial, [(DMF)H]OTf (285.7 mg, 1.281 mmol) was dissolved in 240 μL of MeCN. Aliquots of 50 μL were transferred by syringe to the cell solution, and a CV was recorded after each addition. The working electrode was polished prior to each CV. Acid solution was added until the current no longer increased, whereupon water was

dx.doi.org/10.1021/ic500701a | Inorg. Chem. 2014, 53, 6875−6885

added in 5 μL increments, again until the current no longer increased. The scan rate was 0.05 V s^{-1} for all runs.

Preparation of 1,2,3-Triazolyllithium-Terminated Glassy Carbon Surfaces. Preconditioned glassy carbon samples were modified with 1,2,3-triazolyllithium terminal groups by reaction first with $[Bu_4N][Cl-I-N_3]$ and then with (en)Li≡CH as described previously,[16] except with approximately 25 mg rather than 100 mg of (en)Li≡CH in 2 mL of THF used for the second step. (en)Li≡CH is fully soluble at this loading, and much less residual Li was detected by XPS following the coupling step.

Coupling with $Ni^0(P^{Ph}_2N^{ArNHS}_2)_2$ and $[(MeCN)Ni^{II}(P^{Ph}_2N^{ArNHS}_2)_2](BF_4)_2$. In a typical experiment, $Ni^0(P^{Ph}_2N^{ArNHS}_2)_2$ (14.7 mg, 8.9 μmol) was dissolved in 1 mL of THF in a screw-cap vial containing a stirbar. A freshly prepared 1,2,3-triazolyllithium-terminated electrode was fitted into the vial through a septum cap, held with stirring for 18 h, and then rinsed with THF. The electrode was then shaken for 1 min with 10/1 THF/water. To ensure the removal of adsorbates, the electrode was held in a stirred 1/1 THF/MeCN solution for 15 min. The electrode was then rinsed again with THF and used directly for CV measurements. A similar procedure was used for coupling with $[(MeCN)Ni^{II}(P^{Ph}_2N^{ArNHS}_2)_2](BF_4)_2$ (16.5 mg, 9.3 μmol). Material quantities were increased 5-fold for the modification of glassy carbon plate samples.

Electrochemical Measurements with Electrodes Modified with $Ni^0(P^{Ph}_2N^{ArNHS}_2)_2$ and $[(MeCN)Ni^{II}(P^{Ph}_2N^{ArNHS}_2)_2](BF_4)_2$. The modified electrode was placed in an electrochemical cell containing 2 mL of MeCN (0.1 M $[Bu_4N]PF_6$). Fc was added, and the required CV experiments were performed. Starting potentials were positive of the Ni(II/I) couple of the parent complex with the Ni(II)-modified electrodes and negative of the Ni(I/0) couple with Ni(0)-modified electrodes.

Electrocatalysis with Modified Electrodes. In a typical experiment, an electrode modified with $Ni^0(P^{Ph}_2N^{ArNHS}_2)_2$ was placed in an electrochemical cell containing 2 mL of MeCN (0.1 M $[Bu_4N]PF_6$). Fc was added, and a cyclic voltammogram was recorded. In a separate vial, [(DMF)H]OTf (446.1 mg, 2.00 mmol) was dissolved in 2.0 mL of MeCN. Aliquots of 50 μL were transferred by syringe to the cell solution, and a CV was recorded after each addition. Acid solution was added until the current no longer increased. The scan rate was 0.05 V s^{-1} for all runs. Experiments using electrodes modified with $[(MeCN)Ni^{II}(P^{Ph}_2N^{ArNHS}_2)_2](BF_4)_2$ were conducted in a similar fashion (see Figure S8 of the Supporting Information).

■ ASSOCIATED CONTENT

Ⓢ Supporting Information

Figures giving voltammetric and X-ray photoelectron spectroscopic data. This material is available free of charge via the Internet at http://pubs.acs.org.

■ AUTHOR INFORMATION

Corresponding Author

*E-mail for J.A.S.R.: john.roberts@pnnl.gov.

Notes

The authors declare no competing financial interest.

■ ACKNOWLEDGMENTS

This research was supported as part of the Center for Molecular Electrocatalysis, an Energy Frontier Research Center funded by the US Department of Energy, Office of Science, Office of Basic Energy Sciences. Pacific Northwest National Laboratory is operated by Battelle for the US Department of Energy. The XPS measurements were performed at EMSL, a national scientific user facility sponsored by the Department of Energy's Office of Biological and Environmental Research and located at Pacific Northwest National Laboratory.

■ REFERENCES

(1) (a) Dempsey, J. L.; Brunschwig, B. S.; Winkler, J. R.; Gray, H. B. *Acc. Chem. Res.* **2009**, *42*, 1995−2004. (b) Rakowski DuBois, M.; DuBois, D. L. *Chem. Soc. Rev.* **2009**, *38*, 62−72. (c) Benson, E. E.; Kubiak, C. P.; Sathrum, A. J.; Smieja, J. M. *Chem. Soc. Rev.* **2009**, *38*, 89−99. (d) Liu, T.; DuBois, D. L.; Bullock, R. M. *Nat. Chem.* **2013**, *5*, 228−233. (e) McNamara, W. R.; Han, Z.; Yin, C.-J.; Brennessel, W. W.; Holland, P. L.; Eisenberg, R. *Proc. Natl. Acad. Sci. U.S.A.* **2012**, *109*, 15594−15599. (f) Bullock, R. M.; Appel, A. M.; Helm, M. L. *Chem. Commun.* **2014**, *50*, 3125−3143. (g) Ogo, S. *Chem. Commun.* **2009**, 3317−3325.

(2) (a) Anfuso, C. L.; Snoeberger, R. C.; Ricks, A. M.; Liu, W.; Xiao, D.; Batista, V. S.; Lian, T. *J. Am. Chem. Soc.* **2011**, *133*, 6922−6925. (b) Blakemore, J. D.; Gupta, A.; Warren, J. J.; Brunschwig, B. S.; Gray, H. B. *J. Am. Chem. Soc.* **2013**, *135*, 18288−18291.

(3) (a) Chen, Z.; Concepcion, J. J.; Hull, J. F.; Hoertz, P. G.; Meyer, T. J. *Dalton Trans.* **2010**, *39*, 6950−6952. (b) Tong, L.; Gothelid, M.; Sun, L. *Chem. Commun.* **2012**, *48*, 10025−10027.

(4) (a) Yao, S. A.; Ruther, R. E.; Zhang, L.; Franking, R. A.; Hamers, R. J.; Berry, J. F. *J. Am. Chem. Soc.* **2012**, *134*, 15632−15635. (b) Krawicz, A.; Yang, J.; Anzenberg, E.; Yano, J.; Sharp, I. D.; Moore, G. F. *J. Am. Chem. Soc.* **2013**, *135*, 11861−11868.

(5) McCrory, C. C. L.; Devadoss, A.; Ottenwaelder, X.; Lowe, R. D.; Stack, T. D. P.; Chidsey, C. E. D. *J. Am. Chem. Soc.* **2011**, *133*, 3696−3699.

(6) (a) Le Goff, A.; Artero, V.; Jousselme, B.; Tran, P. D.; Guillet, N.; Métayé, R.; Fihri, A.; Palacin, S.; Fontecave, M. *Science* **2009**, *326*, 1384−1387. (b) Tran, P. D.; Le Goff, A.; Heidkamp, J.; Jousselme, B.; Guillet, N.; Palacin, S.; Dau, H.; Fontecave, M.; Artero, V. *Angew. Chem., Int. Ed.* **2011**, *50*, 1371−1374.

(7) (a) Gross, M. A.; Reynal, A.; Durrant, J. R.; Reisner, E. *J. Am. Chem. Soc.* **2014**, *136*, 356−366. (b) Moore, G. F.; Sharp, I. D. *J. Phys. Chem. Lett.* **2013**, *4*, 568−572. (c) Silver, S. C.; Niklas, J.; Du, P.; Poluektov, O. G.; Tiede, D. M.; Utschig, L. M. *J. Am. Chem. Soc.* **2013**, *135*, 13246−13249.

(8) (a) Kilgore, U. J.; Roberts, J. A. S.; Pool, D. H.; Appel, A. M.; Stewart, M. P.; DuBois, M. R.; Dougherty, W. G.; Kassel, W. S.; Bullock, R. M.; DuBois, D. L. *J. Am. Chem. Soc.* **2011**, *133*, 5861−5872. (b) Kilgore, U. J.; Stewart, M. P.; Helm, M. L.; Dougherty, W. G.; Kassel, W. S.; DuBois, M. R.; DuBois, D. L.; Bullock, R. M. *Inorg. Chem.* **2011**, *50*, 10908−10918.

(9) (a) DuBois, D. L.; Bullock, R. M. *Eur. J. Inorg. Chem.* **2011**, *2011*, 1017−1027. (b) O'Hagan, M.; Shaw, W. J.; Raugei, S.; Chen, S.; Yang, J. Y.; Kilgore, U. J.; DuBois, D. L.; Bullock, R. M. *J. Am. Chem. Soc.* **2011**, *133*, 14301−14312.

(10) (a) *Catalysis without Precious Metals*; Bullock, R. M., Ed.; Wiley-VCH: Weinheim, Germany, 2010. (b) Wang, M.; Chen, L.; Sun, L. *Energy Environ. Sci.* **2012**, *5*, 6763−6778. (c) Thoi, V. S.; Sun, Y.; Long, J. R.; Chang, C. J. *Chem. Soc. Rev.* **2013**, *42*, 2388−2400.

(11) (a) Pool, D. H.; Stewart, M. P.; O'Hagan, M.; Shaw, W. J.; Roberts, J. A. S.; Bullock, R. M.; DuBois, D. L. *Proc. Natl. Acad. Sci. U.S.A.* **2012**, *109*, 15634−15639. (b) Hoffert, W. A.; Roberts, J. A. S.; Bullock, R. M.; Helm, M. L. *Chem. Commun.* **2013**, *49*, 7767−7769. (c) Helm, M. L.; Stewart, M. P.; Bullock, R. M.; DuBois, M. R.; DuBois, D. L. *Science* **2011**, *333*, 863−866.

(12) This is the current density generated by illuminating a photovoltaic device with unfocused sunlight, see: McFarlane, S. L.; Day, B. A.; McEleney, K.; Freund, M. S.; Lewis, N. S. *Energy Environ. Sci.* **2011**, *4*, 1700−1703.

(13) Cook, T. R.; Dogutan, D. K.; Reece, S. Y.; Surendranath, Y.; Teets, T. S.; Nocera, D. G. *Chem. Rev.* **2010**, *110*, 6474−6502.

(14) Favier, I.; Duñach, E. *Tetrahedron Lett.* **2004**, *45*, 3393−3395.

(15) Roberts, J. A. S.; Bullock, R. M. *Inorg. Chem.* **2013**, *52*, 3823−3835.

(16) Das, A. K.; Engelhard, M. H.; Liu, F.; Bullock, R. M.; Roberts, J. A. S. *Inorg. Chem.* **2013**, *52*, 13674−13684.

(17) Laviron, E. *J. Electroanal. Chem.* **1979**, *101*, 19−28.

(18) Grosvenor, A. P.; Biesinger, M. C.; Smart, R. S. C.; McIntyre, N. S. *Surf. Sci.* **2006**, *600*, 1771−1779.

(19) (a) Yang, G.; Hu, H.; Zhou, Y.; Hu, Y.; Huang, H.; Nie, F.; Shi, W. *Sci. Rep.* **2012**, DOI: 10.1038/srep00698. (b) Peng, H.; Mo, Z.; Liao, S.; Liang, H.; Yang, L.; Luo, F.; Song, H.; Zhong, Y.; Zhang, B. *Sci. Rep.* **2013**, DOI: 10.1038/srep01765.
(20) Devadoss, A.; Chidsey, C. E. D. *J. Am. Chem. Soc.* **2007**, *129*, 5370−5371.
(21) (a) Kim, K. S.; Winograd, N. *Surf. Sci.* **1974**, *43*, 625−643. (b) Selvam, P.; Viswanathan, B.; Srinivasan, V. *J. Electron Spectrosc. Relat. Phenom.* **1989**, *49*, 203−211.
(22) (a) Ruther, R. E.; Cui, Q.; Hamers, R. J. *J. Am. Chem. Soc.* **2013**, *135*, 5751−5761. (b) Seah, M. In *Surface Analysis by Auger and X-ray Photoelectron Spectroscopy*; Briggs, D., Grant, J. T., Eds.; IM Publications: Chichester, U.K., 2003. (c) Powell, C. J.; Seah, M. P. *J. Vac. Sci. Technol., A* **1990**, *8*, 735−763.
(23) Fang, M.; Engelhard, M. H.; Zhu, Z.; Helm, M. L.; Roberts, J. A. S. *ACS Catal.* **2013**, *4*, 90−98.
(24) The onset potential is identified as the potential at which a line extending the baseline toward more negative potentials intersects a line extending the catalytic current response toward the zero current axis.
(25) Wilson, A. D.; Newell, R. H.; McNevin, M. J.; Muckerman, J. T.; DuBois, M. R.; DuBois, D. L. *J. Am. Chem. Soc.* **2006**, *128*, 358−366.
(26) Sathrum, A. J.; Kubiak, C. P. *J. Phys. Chem. Lett.* **2011**, *2*, 2372−2379.
(27) (a) Kolthoff, I. M.; Chantooni, M. K.; Bhowmik, S. *Anal. Chem.* **1967**, *39*, 1627−1633. (b) Izutsu, K. *Acid-Base Dissociation Constants in Dipolar Aprotic Solvents*; Pergamon Press: Oxford, U.K., 1990.
(28) Kaljurand, I.; Kutt, A.; Soovali, L.; Rodima, T.; Maemets, V.; Leito, I.; Koppel, I. A. *J. Org. Chem.* **2005**, *70*, 1019−1028.
(29) Artero, V.; Fontecave, M. *Chem. Soc. Rev.* **2013**, *42*, 2338−2356.
(30) (a) Krasiński, A.; Fokin, V. V.; Sharpless, K. B. *Org. Lett.* **2004**, *6*, 1237−1240. (b) Akimova, G. S.; Chistokletov, V. N.; Petrov, A. A. *Zh. Org. Khim.* **1967**, *3*, 968−974. (c) Akimova, G. S.; Chistokletov, V. N.; Petrov, A. A. *Zh. Org. Khim.* **1967**, *3*, 2241−2247. (d) Akimova, G. S.; Chistokletov, V. N.; Petrov, A. A. *Zh. Org. Khim.* **1968**, *4*, 389−394.
(31) Anariba, F.; DuVall, S. H.; McCreery, R. L. *Anal. Chem.* **2003**, *75*, 3837−3844.
(32) Pinson, J.; Podvorica, F. *Chem. Soc. Rev.* **2005**, *34*, 429−439.
(33) Bream, R. N.; Hayes, D.; Hulcoop, D. G.; Whiteman, A. J. *Org. Process Res. Dev.* **2013**, *17*, 641−650.
(34) Fontecave, M.; Artero, V. *C. R. Chim.* **2011**, *14*, 362−371.
(35) Yang, J. Y.; Chen, S.; Dougherty, W. G.; Kassel, W. S.; Bullock, R. M.; DuBois, D. L.; Raugei, S.; Rousseau, R.; Dupuis, M.; Rakowski DuBois, M. *Chem. Commun.* **2010**, *46*, 8618−8620.
(36) (a) Jain, A.; Lense, S.; Linehan, J. C.; Raugei, S.; Cho, H.; DuBois, D. L.; Shaw, W. J. *Inorg. Chem.* **2011**, *50*, 4073−4085. (b) Galan, B. R.; Schöffel, J.; Linehan, J. C.; Seu, C.; Appel, A. M.; Roberts, J. A. S.; Helm, M. L.; Kilgore, U. J.; Yang, J. Y.; DuBois, D. L.; Kubiak, C. P. *J. Am. Chem. Soc.* **2011**, *133*, 12767−12779.
(37) Wilson, A. D.; Fraze, K.; Twamley, B.; Miller, S. M.; DuBois, D. L.; Rakowski DuBois, M. *J. Am. Chem. Soc.* **2007**, *130*, 1061−1068.
(38) Franz, J. A.; O'Hagan, M.; Ho, M. H.; Liu, T.; Helm, M. L.; Lense, S.; DuBois, D. L.; Shaw, W. J.; Appel, A. M.; Raugei, S.; Bullock, R. M. *Organometallics* **2013**, *32*, 7034−7042.
(39) Chen, S.; Ho, M.-H.; Bullock, R. M.; DuBois, D. L.; Dupuis, M.; Rousseau, R.; Raugei, S. *ACS Catal.* **2013**, *4*, 229−242.
(40) (a) Yang, J. Y.; Bullock, R. M.; Dougherty, W. G.; Kassel, W. S.; Twamley, B.; DuBois, D. L.; Rakowski DuBois, M. *Dalton Trans.* **2010**, *39*, 3001−3010. (b) Wiedner, E. S.; Yang, J. Y.; Chen, S.; Raugei, S.; Dougherty, W. G.; Kassel, W. S.; Helm, M. L.; Bullock, R. M.; Rakowski DuBois, M.; DuBois, D. L. *Organometallics* **2011**, *31*, 144−156.
(41) The catalyst concentration gradient is 0 with a well-mixed solution. However, even if 100% of the surface Ni species were released as active catalysts, the electrode surface carries far too few Ni molecules to produce a measurable response.
(42) Savéant, J. M. *Elements of molecular and biomolecular electrochemistry: an electrochemical approach to electron transfer chemistry.*; Wiley: Hoboken, NJ, 2006.
(43) Raugei, S.; Chen, S.; Ho, M.-H.; Ginovska-Pangovska, B.; Rousseau, R. J.; Dupuis, M.; DuBois, D. L.; Bullock, R. M. *Chem. Eur. J.* **2012**, *18*, 6493−6506.
(44) (a) O'Hagan, M.; Shaw, W. J.; Raugei, S.; Chen, S. T.; Yang, J. Y.; Kilgore, U. J.; DuBois, D. L.; Bullock, R. M. *J. Am. Chem. Soc.* **2011**, *133*, 14301−14312. (b) O'Hagan, M.; Ho, M. H.; Yang, J. Y.; Appel, A. M.; Rawkowski DuBois, M.; Raugei, S.; Shaw, W. J.; DuBois, D. L.; Bullock, R. M. *J. Am. Chem. Soc.* **2012**, *134*, 19409−19424.
(45) Sirkar, K. K. *Separation of molecules, macromolecules, and particles: principles, phenomena, and processes*; Cambridge University Press: Cambridge, U.K., 2014.
(46) Yang, J. Y.; Bullock, R. M.; Shaw, W. J.; Twamley, B.; Fraze, K.; Rakowski DuBois, M.; DuBois, D. L. *J. Am. Chem. Soc.* **2009**, *131*, 5935−5945.
(47) Fraze, K.; Wilson, A. D.; Appel, A. M.; Rakowski DuBois, M.; DuBois, D. L. *Organometallics* **2007**, *26*, 3918−3924.
(48) C. Davies, S.; A. Henderson, R.; L. Hughes, D.; E. Oglieve, K. *J. Chem. Soc., Dalton Trans.* **1998**, 425−432.
(49) Fry, A. J. In *Laboratory Techniques in Electroanalytical Chemistry*, 2nd ed.; Kissinger, P. T., Heineman, W. R., Eds.; Marcel Dekker: New York, 1996; pp 469−483.
(50) Hathaway, B. J.; Holah, D. G.; Underhill, A. E. *J. Chem. Soc.* **1962**, 2444−2448.
(51) Reback, M. L.; Ginovska-Pangovska, B.; Ho, M.-H.; Jain, A.; Squier, T. C.; Raugei, S.; Roberts, J. A. S.; Shaw, W. J. *Chem. Eur. J.* **2013**, *19*, 1928−1941.
(52) Gelius, U.; Allan, C. J.; Johansson, G.; Siegbahn, H.; Allison, D. A.; Siegbahn, K. *Phys. Scr.* **1971**, *3*, 237.
(53) Estrade-Szwarckopf, H.; Rousseau, B. *J. Phys. Chem. Solids* **1992**, *53*, 419−436.